

Electron spin resonance study of polycrystalline  $\text{La}_{0.75}(\text{Ca}_x\text{Sr}_{1-x})_{0.25}\text{MnO}_3$  ( $x = 0, 0.45, 1$ )

This article has been downloaded from IOPscience. Please scroll down to see the full text article.

2009 J. Phys.: Condens. Matter 21 046002

(<http://iopscience.iop.org/0953-8984/21/4/046002>)

View [the table of contents for this issue](#), or go to the [journal homepage](#) for more

Download details:

IP Address: 129.252.86.83

The article was downloaded on 29/05/2010 at 17:31

Please note that [terms and conditions apply](#).

# Electron spin resonance study of polycrystalline $\text{La}_{0.75}(\text{Ca}_x\text{Sr}_{1-x})_{0.25}\text{MnO}_3$ ( $x = 0, 0.45, 1$ )

H P Yang, L Shi<sup>1</sup>, S M Zhou, J Y Zhao, L F He and Y B Jia

Hefei National Laboratory for Physical Sciences at the Microscale, University of Science and Technology of China, Hefei, Anhui 230026, People's Republic of China

E-mail: [shil@ustc.edu.cn](mailto:shil@ustc.edu.cn)

Received 30 July 2008, in final form 18 November 2008

Published 19 December 2008

Online at [stacks.iop.org/JPhysCM/21/046002](http://stacks.iop.org/JPhysCM/21/046002)

## Abstract

Electron spin resonance (ESR) spectra of polycrystalline  $\text{La}_{0.75}(\text{Ca}_x\text{Sr}_{1-x})_{0.25}\text{MnO}_3$  ( $x = 0, 0.45, 1$ ) were studied within the temperature range  $110 \text{ K} \leq T \leq 470 \text{ K}$ . The temperature dependence of the ESR intensity for the samples is described by a thermally activated model in the paramagnetic regime. It is found that the activation energy in the orthorhombic phase is higher than that in the rhombohedral phase for  $\text{La}_{0.75}(\text{Ca}_{0.45}\text{Sr}_{0.55})_{0.25}\text{MnO}_3$ . It is suggested that a higher energy is required to destroy the correlated polarons due to the fact that correlated polarons only exist in the orthorhombic phase. This proposition is confirmed by the analysis of the ESR linewidth data, which can be well fitted by the model of adiabatic hopping motion of small polarons. In addition, it is found that, at a fixed temperature, the linewidth decreases with increasing Sr doping, which reveals that the structural tolerance factor has a significant effect on the linewidth.

(Some figures in this article are in colour only in the electronic version)

## 1. Introduction

Manganites  $\text{R}_{1-x}\text{A}_x\text{MnO}_3$  ( $\text{R} = \text{La}, \text{Pr}, \text{Nd}, \text{etc.}$  and  $\text{A} = \text{Ca}, \text{Sr}, \text{Ba}, \text{Pb}, \text{etc.}$ ) have attracted a great deal of interest because of the colossal magnetoresistance effect (CMR). The CMR effect usually appears in the vicinity of the transition from a paramagnetic insulating state (PI) to a ferromagnetic metallic state (FMM). The ferromagnetic metallic state is conventionally explained by the double exchange (DE) model [1], where the hopping of an itinerant  $e_g$  electron from the trivalent  $\text{Mn}^{3+}$  to the tetravalent  $\text{Mn}^{4+}$  site facilitates both ferromagnetism and electrical conductivity. However, the model is not adequate to explain the high resistivity of the PI state and the physical properties of the PI state are still unclear now [2].

Recently, a great deal of theoretical and experimental work has revealed that nanoscale lattice polarons resulting from electron–phonon coupling via the Jahn–Teller active  $\text{Mn}^{3+}$  play a key role in the manganites [2–5]. Pulsed neutron diffraction research of polycrystalline  $\text{La}_{1-x}\text{Sr}_x\text{MnO}_3$

observed local lattice distortions arising from the Jahn–Teller interaction and the lattice distortions are related to the polarons [3]. A single, isolated lattice polaron forms when an  $e_g$  electron localizes on an  $\text{Mn}^{3+}$  site to minimize the energy, and the surrounding  $\text{Mn}^{3+}\text{O}_6$  octahedron distorts due to the Jahn–Teller interaction. Nanoscale structural correlations with a correlation length of several lattice constants have been observed by synchrotron x-ray and neutron diffraction experiments [5]. The structural correlations contribute to the interaction of polarons through the overlapping long-range lattice distortions and a correlated polaron develops. The development of correlation between polarons seems to be related to the formation of a charge ordering state [6]. The presence of the correlated and uncorrelated Jahn–Teller (JT) polarons was detected in the paramagnetic phase of several manganite samples by x-ray and neutron scattering studies [5–7]. However, based on our knowledge, up to now, there is no report about the typical value of the polaron correlation energy. To elucidate the realistic structure of the correlated regions and the physics of polarons, more experiments are needed.

<sup>1</sup> Author to whom any correspondence should be addressed.

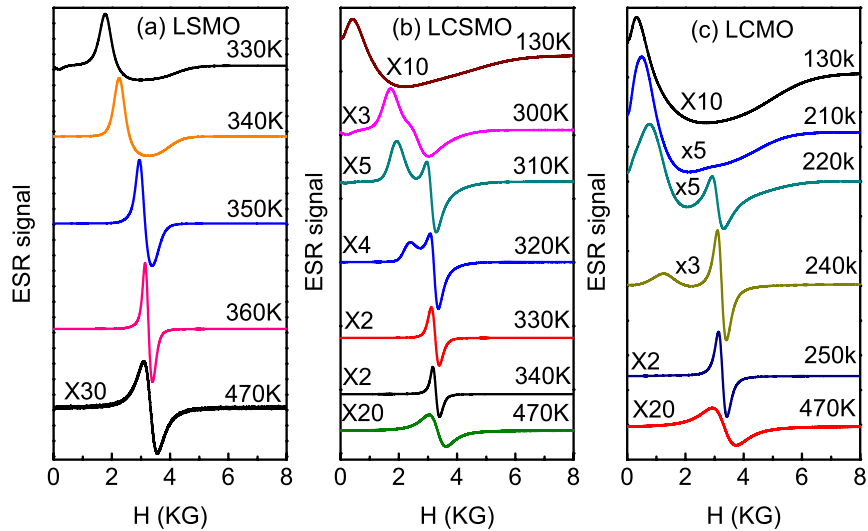


**Figure 1.** Temperature dependence of ESR spectra: (a) LSMO, (b) LCSMO, (c) LCMO.

Recently, x-ray and neutron scattering measurements of single-crystalline  $\text{La}_{0.75}(\text{Ca}_{0.45}\text{Sr}_{0.55})_{0.25}\text{MnO}_3$ , which undergoes a transition from an orthorhombic state to a rhombohedral state in the paramagnetic region, have established that the uncorrelated polarons are present in both orthorhombic and rhombohedral phases, while the correlated polarons only exist in the orthorhombic phase [8]. Kiryukhin *et al* proved by the analysis of electronic bandwidth that the structural change has a negligible effect on the transport properties and the larger electrical resistivity in the orthorhombic state for  $\text{La}_{0.75}(\text{Ca}_{0.45}\text{Sr}_{0.55})_{0.25}\text{MnO}_3$  was attributed to the presence of the correlated polarons [8, 9]. However, the magnetic behaviors of the correlated and uncorrelated polarons have been less investigated so far. On the other hand, it is well known that electron spin resonance (ESR) is a powerful technique to study the static and dynamic magnetic correlations of manganese perovskites [10–13].

In this work, polycrystalline  $\text{La}_{0.75}(\text{Ca}_x\text{Sr}_{1-x})_{0.25}\text{MnO}_3$  ( $x = 0, 0.45, 1$ ) samples were measured by the ESR method to study the spin dynamics of the polarons. A detailed investigation of the temperature dependence of the intensity, ESR linewidth and resonance field for  $\text{La}_{0.75}(\text{Ca}_x\text{Sr}_{1-x})_{0.25}\text{MnO}_3$  ( $x = 0, 0.45, 1$ ) was reported. The temperature dependence of the intensity in the PM regime was analyzed by a thermally activated model. It was found that the activation energy in the orthorhombic phase is higher than that in the rhombohedral phase for  $\text{La}_{0.75}(\text{Ca}_{0.45}\text{Sr}_{0.55})_{0.25}\text{MnO}_3$ . It is suggested that a higher energy is required to destroy the correlated polarons.

## 2. Experimental details

The polycrystalline samples of  $\text{La}_{0.75}(\text{Ca}_x\text{Sr}_{1-x})_{0.25}\text{MnO}_3$  ( $x = 0, 0.45, 1$ ) were synthesized by a conventional solid-state reaction (SSR) method. The stoichiometric amounts of high-purity  $\text{La}_2\text{O}_3$ ,  $\text{SrCO}_3$ ,  $\text{CaCO}_3$  and  $\text{MnO}_2$  powders were mixed and pre-sintered at  $950^\circ\text{C}$  for 14 h, and then repeatedly ground and heated at  $1200^\circ\text{C}$  and  $1300^\circ\text{C}$  for 24 h and 48 h,

respectively. After grinding, the mixture was pressed into pellets and sintered at  $1350^\circ\text{C}$  for 36 h. The crystal structure and phase purity were determined by an 18 kW rotating anode x-ray diffractometer (XRD, Type MXP18AHF, MAC science) to ensure getting pure final products. ESR spectra were taken with a JES-FA 200 spectrometer at 9.06 GHz. The measurements were performed on small loose-packed powders (about 5 mg).

## 3. Results and discussion

X-ray diffraction patterns indicate that the structures of  $\text{La}_{0.75}\text{Ca}_{0.25}\text{MnO}_3$  (LCMO) and  $\text{La}_{0.75}(\text{Ca}_{0.45}\text{Sr}_{0.55})_{0.25}\text{MnO}_3$  (LCSMO) are orthorhombic, while  $\text{La}_{0.75}\text{Sr}_{0.25}\text{MnO}_3$  (LSMO) is rhombohedral at room temperature. From high temperature x-ray diffraction studies of LCSMO, it is found that, upon increasing temperature, there is a structural transition from the orthorhombic phase to rhombohedral phase at  $T_S \approx 355$  K, which coincides with the results reported by Kiryukhin *et al* [8, 9].

The ESR spectra at some representative temperatures for LCMO, LSMO and LCSMO are shown in figure 1. From figure 1, it can be seen that for LSMO, at high temperatures above  $T_C \approx 360$  K, the ESR spectrum consists of a single Lorentzian line with a  $g$  factor value near to 2.00. Below 360 K, an obvious asymmetric ESR signal appears and the signal shifts to lower resonance field with decreasing temperature due to the FM double exchange between  $\text{Mn}^{3+}$  and  $\text{Mn}^{4+}$  ions. For LCMO, above 250 K, the ESR spectrum is characteristic of a PM signal. Below this temperature, the ESR signal splits into two lines with decreasing temperature: one has the PM characteristic and the other one shifts to lower field upon cooling, which shows the character of FM resonance. Study of LCMO by Ccahuana *et al* [14] revealed that the coexistence of PM and FM resonances is due to the short-range FM order, and this phenomenon is referred to as a Griffiths phase. The temperature below which FM and PM resonances begin to coexist is defined as  $T_G$  [14, 15]. Below

**Table 1.** The experimental and fitting parameters for LCMO, LSMO and LCSMO. (Note:  $T_C$  and  $T_G$  are defined as the same with [10];  $T_{\min}$  corresponds to the narrowest linewidth;  $E_{a1}$  and  $E_{a2}$  are the fitting parameters of equations (1) and (3), respectively.)

Sample	$T_C$ (K)	$T_{\min}$ (K)	$E_{a1}$ (eV)	$E_{a2}$ (eV)	$f$
LCMO	220	260	$0.108 \pm 0.0006$	$0.106 \pm 0.001$	0.9662
LSMO	360	370	$0.220 \pm 0.004$	$0.149 \pm 0.007$	0.9749
LCSMO (345–370 K)	310	340	$0.243 \pm 0.002$	$0.394 \pm 0.003$	0.9711
LCSMO (390–470 K)			$0.181 \pm 0.001$	$0.124 \pm 0.004$	

$T_C \approx 220$  K, PM resonance disappears and the FM resonance signal shifts to lower field with decreasing temperature, as shown in figure 1(c). The above ESR results of LCMO are consistent with the reports of Ccahuana *et al* [14]. For LCSMO, a similar phenomenon to that of LCMO can be seen in the ESR spectra. Magnetization measurements on  $\text{La}_{2/3}(\text{Ca}_{1-x}\text{Sr}_x)_{1/3}\text{MnO}_3$  with different doping by Rivadulla *et al* revealed a Griffiths phase in their samples [16]. In this work, by the same consideration, it is proposed that, for the polycrystalline LCSMO sample, the coexistence of FM and PM resonances may connect with the Griffiths phase. From figure 1(b), the  $T_C$  of LCSMO is about 310 K and  $T_G$  is about 330 K. The values of  $T_C$  for all samples are summarized in table 1.

The intensities of the ESR spectra for the three samples can be obtained by double integration of the derivative spectra. It is well known that, within the PM regime for the manganites, the ESR intensity  $I(T)$  can be described by a thermally activated model, i.e. the Arrhenius law:

$$I(T) = I_0 \exp\left(-\frac{E_{a1}}{k_B T}\right) \quad (1)$$

where  $I_0$  is a constant,  $k_B$  is the Boltzmann factor and  $E_{a1}$  is the activation energy for the dissociation of FM clusters [17]. The experimental data and the linear fitting curves (solid lines) of  $\ln(I)$  versus  $1000/T$  are plotted in figure 2. As shown in figure 2, for LCMO and LSMO, the data can be well fitted with a straight line in the temperature range above about  $1.1T_C$  using equation (1).  $E_{a1}$  values obtained by the fitting are shown in table 1. It can be seen that the activation energy of LSMO is higher than that of LCMO. Liu *et al* [12] have studied the spin dynamics of  $\text{La}_{1-x}\text{Ca}_x\text{MnO}_3$  with different Ca doping by ESR spectra. By fitting the intensity they found that the activation energy  $E_a$  values display a peak at  $x = 3/8$  where the FM coupling is the strongest. It is proposed that a large activation energy was required to disrupt the spin alignment of adjacent  $\text{Mn}^{3+}$  and  $\text{Mn}^{4+}$  ions due to the strong DE interaction [12]. ESR spectrum investigation of polycrystalline  $\text{La}_{1-x}\text{Pb}_x\text{MnO}_3$  ( $0.1 \leq x \leq 0.5$ ) samples by Phan *et al* has revealed the same phenomenon [13]. As it is known that the DE interaction energy in LSMO is stronger than that in LCMO, to break this strong interaction a higher energy is required. For LCSMO, the data cannot be fitted by one straight line, and two straight lines with different slopes were used to fit the data. As can be seen in figure 2, the data can be well fitted with two straight lines with a crossover at  $T \approx 380$  K. The fitting values of the data in two different regimes are shown in table 1. It can be seen that the fitting value  $E_{a1}$  in the orthorhombic phase is higher than the value  $E_{a1}$  in the rhombohedral phase. It is established that

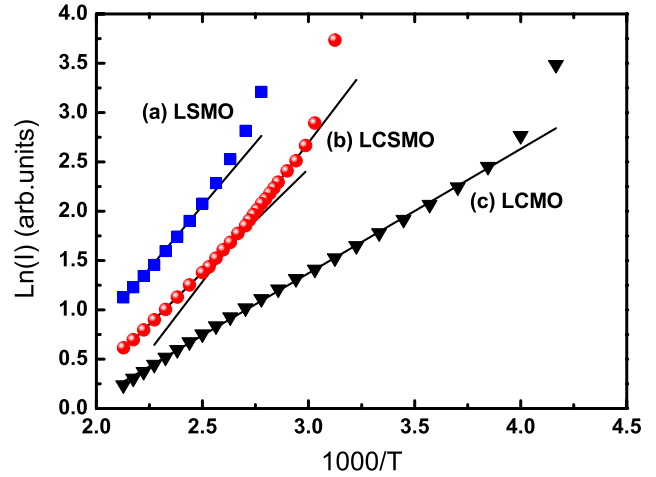


**Figure 2.** Experimental and fitting plots of  $\ln(I)$  versus  $1000/T$  for LSMO, LCSMO and LCMO.

the correlated polarons are present only in the orthorhombic phase [8, 9]. The formation of the correlated polarons is due to the interaction of the polarons with each other through long-range lattice distortions. However, the correlated polarons are absent in the rhombohedral phase. The bonds of the correlated polarons are destroyed, while the structure changes from the orthorhombic phase to the rhombohedral phase. It is suggested that to destroy the interaction of the correlated polarons a higher energy is required, which leads to a higher  $E_{a1}$  value in the orthorhombic phase than in the rhombohedral phase.

It is reported that the ESR spectra in the paramagnetic regime can be fitted by the form including both absorption and dispersion [12, 13]. In this work, however, it is found that the resonance line can also be well fitted by an equation including Lorentz and Gauss lines, which can be expressed as follows [18]:

$$\frac{dP}{dH} \propto \frac{d}{dH} \left[ \alpha \frac{\Delta H}{4(H - H_r)^2 + \Delta H^2} + (1 - \alpha) \frac{1}{\Delta H} \exp\left(-2\frac{(H - H_r)^2}{\Delta H^2}\right) \right] \quad (2)$$

where  $\alpha$  denotes the ratio of the Lorentzian shape part,  $H_r$  is the resonance field and  $\Delta H$  is the linewidth. The temperature dependence of the ESR linewidth  $\Delta H$  is shown in figure 3. It can be seen that the linewidth gradually decreases with decreasing temperature. On approaching  $T_C$  from high temperature,  $\Delta H(T)$  goes through the narrowest value at  $T_{\min} > T_C$ . Below  $T_{\min}$ , the linewidth increases rapidly because of the development of FM correlations [13]. The temperature  $T_{\min}$  values corresponding to the narrowest

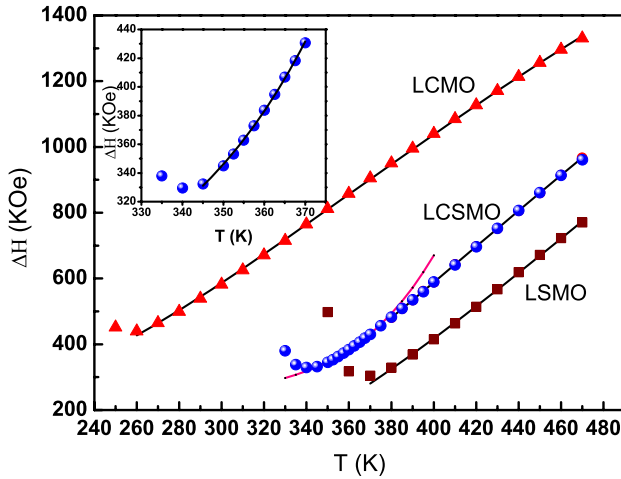


**Figure 3.** Temperature dependence of the ESR linewidth  $\Delta H$  for the samples. Solid lines represent the fitting above  $T_{\min}$  using equation (3). The inset shows the data fitting of LCSMO between 345 and 370 K.

ESR linewidth of the three samples are listed in table 1. Shengelaya *et al* found that the temperature dependence of the ESR linewidth in the paramagnetic regime can be interpreted by the model of adiabatic hopping motion of small polarons, which is consistent with the existence of a bottleneck ESR regime [10]. The model can be expressed by the following equation:

$$\Delta H(T) = \Delta H_0 + \frac{A}{T} \exp\left(-\frac{E_{a2}}{k_B T}\right) \quad (3)$$

where  $\Delta H_0$  and  $A$  are constants, and  $E_{a2}$  is the thermal activation energy. The solid lines in figure 3 represent the fitting of the experimental data. The  $E_{a2}$  values obtained by fitting equation (3) are presented in table 1. For LCSMO, it is found that the thermal activation energy  $E_{a2}$  in the region where orthorhombic phase dominates is higher than that in the rhombohedral phase. The activation energy is thought to be related to short-range correlations of a double exchange origin in mixed-valent  $\text{Mn}^{3+}\text{-Mn}^{4+}$  clusters above  $T_C$  [17]. The higher energy reflects the stronger intercluster interactions. It is established that the correlated polarons are only present in the orthorhombic phase, which is attributed to a higher energy in the orthorhombic phase than that in the rhombohedral phase. The result is similar to the higher  $E_{a1}$  value obtained by fitting of  $\ln(I)$  in the orthorhombic phase, which confirms the supposition that a higher energy is required to dissociate the magnetic interaction in the correlated polarons. For LSMO and LCMO, from the fitting values  $E_{a2}$  it can also be seen that the energy in LSMO is higher than that in LCMO. It can attribute to a stronger DE interaction in LSMO than in LCMO and a higher energy is required to destroy the stronger interaction.

From figure 3, it is found that, at a fixed temperature, the linewidth  $\Delta H$  decreases with increasing Sr doping. By the ESR study of  $\text{Pr}_{0.7}\text{Sr}_{0.3-x}\text{Ca}_x\text{MnO}_3$ , Gundakaram *et al* explained the phenomenon on the basis of the change in the tolerance factor [19]. The tolerance factor  $f$  is defined as  $(r_A + r_O)/\sqrt{2}(r_B + r_O)$ , where  $r_A$ ,  $r_B$  and  $r_O$  are the ionic

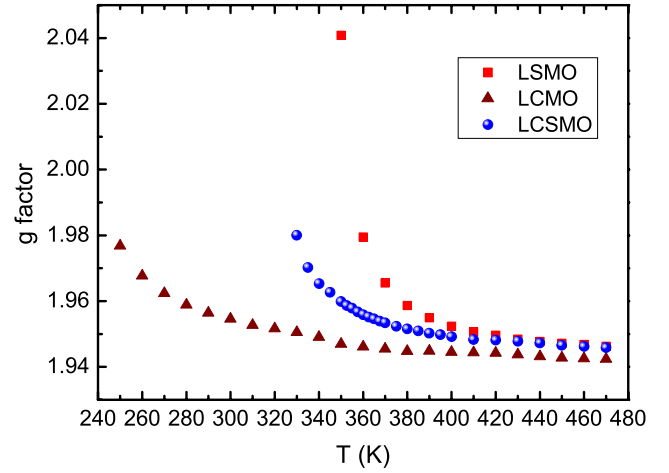


**Figure 4.** Temperature dependence of  $g$  factors for LCMO, LCSMO and LSMO.

radii of the A, B and oxygen ions in the  $\text{ABO}_3$  structure, respectively. The tolerance factors were calculated using the average ionic radii of the samples, as shown in table 1. From table 1, we can see that  $f_{\text{LCMO}} < f_{\text{LCSMO}} < f_{\text{LSMO}}$ , while the linewidth  $\Delta H$  decreases from LCMO to LSMO at the same temperature. These results suggest that the tolerance factor has a significant effect on the linewidth. It is established that the broadening of the ESR linewidth is caused by the spin–lattice relaxation. The hopping rate of the  $e_g$  electrons via the spin–lattice coupling limits the lifetime of the spin state, which leads to a broadening of the ESR linewidth [10, 20]. The increase of the tolerance factor will lead to a decrease of the distortion in the structure, which is supposed to decrease the electron–lattice coupling and the linewidth  $\Delta H$  decreases. To understand how the tolerance factor acts on the ESR linewidth, however, more work is needed.

The resonance field  $H_r$  value can be obtained by fitting the ESR spectrum. The  $g$  factor value was calculated using the equation  $h\nu = g\mu_B H_r$ , where  $h$ ,  $\nu$  and  $\mu_B$  are the Planck constant, microwave frequency and the Bohr magneton, respectively [12, 13]. The temperature dependence of the  $g$  values for the samples are plotted in figure 4. From figure 4, it can be found that, at high temperature in the paramagnetic phase,  $g$  factors are almost temperature-independent. When the temperature decreases near to  $T_C$ , a rapid increase in  $g$  factor can be seen due to the formation of a strong internal field, which shows that FM interaction begins to play an important role in the properties of the samples.

#### 4. Conclusion

In summary, we have probed the magnetic behaviors of polarons by ESR measurements of polycrystalline samples  $\text{La}_{0.75}(\text{Ca}_x\text{Sr}_{1-x})_{0.25}\text{MnO}_3$  ( $x = 0, 0.45, 1$ ). The temperature dependence of the ESR intensity for the samples in the paramagnetic regime is described by a thermally activated model. It is found that the activation energy of  $\text{La}_{0.75}\text{Sr}_{0.25}\text{MnO}_3$  is higher than that of  $\text{La}_{0.75}\text{Ca}_{0.25}\text{MnO}_3$ , which is attributed to the stronger exchange interaction of

$\text{La}_{0.75}\text{Sr}_{0.25}\text{MnO}_3$ . For  $\text{La}_{0.75}(\text{Ca}_{0.45}\text{Sr}_{0.55})_{0.25}\text{MnO}_3$ , it is found that the activation energy in the orthorhombic phase is higher than that in the rhombohedral phase, which is suggested that the correlated polarons only exist in the orthorhombic phase and a higher energy is required to destroy the correlated polarons. This proposition is confirmed by the analysis of the ESR linewidth data, which can be well fitted by the model of adiabatic hopping motion of small polarons. At a fixed temperature the linewidth decreases with increasing Sr doping, which reveals that the tolerance factor has a significant effect on the linewidth. However, more theoretical and experimental work is needed to understand the mechanism of the formation of the correlated and the uncorrelated polarons, and the role the tolerance factor plays in the ESR linewidth.

### Acknowledgments

This project was financially supported by the Ministry of Science and Technology of China (NKBRFSF-G1999064603), the National Basic Research Program of China (973 program, 2009CB939901) and the National Science Foundation of China, grant no. 10874161.

### References

- [1] Zener C 1951 *Phys. Rev.* **82** 403
- [2] Millis A J, Littlewood P B and Shraiman B I 1995 *Phys. Rev. Lett.* **74** 5144
- [3] Despina L, Egami T, Brosha E L, Röder H and Bishop A R 1997 *Phys. Rev. B* **56** R8475
- [4] Mannella N, Rosenhahn A, Booth C H, Marchesini S, Mun B S, Yang S H, Ibrahim K, Tomioka Y and Fadley C S 2004 *Phys. Rev. Lett.* **92** 166401
- [5] Kiryukhin V, Koo T Y, Borissov A, Kim Y J, Nelson C S, Hill J P, Gibbs D and Cheong S-W 2002 *Phys. Rev. B* **65** 094421
- [6] Shimomura S, Wakabayashi N, Kuwahara H and Tokura Y 1999 *Phys. Rev. Lett.* **83** 4389
- [7] Adams C P, Lynn J W, Mukovskii Y M, Arsenov A A and Shulyatev D A 2000 *Phys. Rev. Lett.* **85** 3954
- [8] Kiryukhin V 2004 *New J. Phys.* **6** 155
- [9] Kiryukhin V, Borissov A, Ahn J S, Huang Q, Lynn J W and Cheong S W 2004 *Phys. Rev. B* **70** 214424
- [10] Shengelaya A, Zhao G-M, Keller H, Müller K A and Kochelaev B I 2000 *Phys. Rev. B* **61** 5888
- [11] Angappane S, Pattabiraman M, Rangarajan G, Sethupathi K, Varghese B and Sastry V S 2007 *J. Phys.: Condens. Matter* **19** 036207
- [12] Liu Y, Wan S L and Li X-G 2007 *J. Phys.: Condens. Matter* **19** 196213
- [13] Phan T L, Min S G, Phan M H, Ha N D, Chau N and Yu S C 2007 *Phys. Status Solidi b* **244** 1109
- [14] Ccahuana D L, Winkler E, Prado F, Butera A, Ramos C A, Causa M T and Tovar M 2004 *Physica B* **55–58** 354
- [15] Deisenhofer J, Braak D, Krug von Nidda H-A, Hemberger J, Eremina R M, Ivanshin V A, Balbashov A M, Jug G, Loidl A, Kimura T and Tokura Y 2005 *Phys. Rev. Lett.* **95** 257202
- [16] Rivadulla F, Otero-Leal M, Espinosa A, de-Andrés A, Ramos C, Rivas J and Goodenough J B 2006 *Phys. Rev. Lett.* **96** 016402
- [17] Shames A I, Rozenberg E, McCarroll W H, Greenblatt M and Gorodetsky G 2001 *Phys. Rev. B* **64** 172401
- [18] *The Handbook of JES-FA Series ESR Spectrometer (Simulation)* 2000 (Japan: JEOL)
- [19] Gundakaram R, Lin J G and Huang C Y 1998 *Phys. Rev. B* **58** 12247
- [20] Movaghgar B, Schweitzer L and Overhof H 1978 *Phil. Mag.* **37** 683